Proceedings of the 9ICEG
9th International Congress on Environmental Geotechnics
25-28 June, 2023 | Chania, Greece

https://doi.org/10.53243/ICEG2023-48

Quantification of Different Types of Unfrozen Water Contents in Various Soils by Low-field Nuclear Magnetic Resonance

Y. Wang[1], Y. Wu[1], L. Hu[1]*, and Z. Yin[2]

[1]State Key Laboratory of Hydro-Science and Engineering, Department of Hydraulic Engineering, Tsinghua University, Beijing, China;

[2]Department of Civil and Environmental Engineering, The Hong Kong Polytechnic University, Hong Kong;

**Corresponding author: gehu@tsinghua.edu.cn*

ABSTRACT

A certain amount of liquid water remains in soils at sub-freezing temperatures due to the soil-water interactions. The relationship between unfrozen water content and temperature, i.e., soil freezing characteristic curve (SFCC), governs the hydrologic and mechanical behaviors of soils. Theoretically, different types of water, e.g., adsorptive water and capillary water, exhibit different freezing behaviors and have distinct impacts on the overall properties of freezing soil. In this study, low-field nuclear magnetic resonance (NMR) was utilized to measure the unfrozen water contents of soils with different particle sizes and dry densities. The NMR-measured SFCCs demonstrate that the unfrozen water content is highly dependent on soil properties. The NMR tests show that the T_2 relaxation can identify and quantify different types of soil water. The T_2 distribution results also indicate that the steep drops of unfrozen water contents are primarily caused by supercooling, and the freezing of adsorbed water occurs gradually. A commonly used SFCC model was used to fit the measured data, and the fitting results suggest that the model without consideration of the different types of soil water is insufficient to accurately simulate SFCCs. This study reveals the roles of different types of soil water in the freezing process, providing a basis for a better understanding of the behaviors of freezing soil.

Keywords: Freezing soil; unfrozen water content; NMR; adsorbed water; capillary water

1 INTRODUCTION

The freezing point of soil water is generally lower than that of bulk water due to the complex interactions between soil matrix and water. The relationship between temperature and unfrozen water content in soil is called the soil freezing characteristic curve (SFCC), which plays a significant role in the realm of cold region science and engineering. SFCC governs a series of hydrological and mechanical properties of freezing soil, such as hydraulic conductivity, thermal conductivity, and elastic modulus (Zhang & Lu, 2021). Therefore, estimating the amount of unfrozen water and revealing the mechanisms underlying soil water freezing are of great scientific importance and practical engineering values.

Researchers have found many factors affecting the SFCC, which can be roughly classified into two categories, i.e., experimental conditions and soil properties. The experimental conditions include but are not limited to the freeze-thaw cycles, initial water content, and external loading (Teng et al., 2020). And the soil properties include but are not limited to particle size distribution (PSD), specific surface area (SSA), and clay content (Chen et al., 2021; Tian et al., 2017). The high correlation between these factors and SFCCs has been validated by many studies. However, only a few studies focused on explicating how these factors affect the freezing behaviors of soil water.

Water freezing is a common phenomenon in nature, which can be described by the chemical potential equilibrium. Substance spontaneously transforms from the phase with higher chemical potential to the phase with lower chemical potential. Chemical potential is a function of pressure and temperature for a pure substance, and the chemical potentials of water and ice are equal at the air pressure and 0 °C (Job & Herrmann, 2006). However, the pressure of soil water is not equal to the air pressure due to soil-water interactions. Soil-water interactions can be divided into two types: adsorption and capillarity (Wang et al., 2022b). Adsorption originates from the attractive forces between water molecules and soil matrix, and capillarity describes the capillary condensation in pores due to the surface tension of soil water. The different water retention mechanisms indicate the different physical properties of adsorptive water and capillary water. Adsorptive water mainly exists in the space near the soil particle surface, where the adsorptive forces are strong and cause the local water pressure higher than air pressure. And capillary water mainly exists in the pore space relatively far from the soil surface, where the adsorptive effects are negligible and the local water pressure is controlled by the surface tension and lower than the air pressure. Correspondingly, ice phases at different spatial locations also are affected by adsorption or capillarity. These influences change the pressure within the pore water and pore ice, i.e., change their chemical potential, and depress the freezing point of soil water. Besides adsorptive water and capillary water, bulk water also widely exists in natural soils, which makes the freezing behavior of soil water more complex. Adsorption and capillarity are intrinsically dominated by the soil properties, i.e., clay content, SSA, and PSD, which connect the micro soil properties and macro soil freezing process.

Although the different behaviors of different types of soil water in the soil freezing process have been noticed by researchers, the identification and quantification of different types of soil water are difficult. With the development of experimental technology, low-field nuclear magnetic resonance (NMR) paves a feasible way to identify and quantify the different types of soil water and measure the unfrozen water content. The water molecule is a magnetic needle and can be detected by NMR. Water molecules in different states give different signals to NMR. Hence, the ice, adsorptive water, capillary water, and bulk water can be distinguished from the NMR results (Chen et al., 2021). Nowadays, NMR has been one of the most popular methods to study freezing soil because the NMR test is convenient and will not damage the sample.

In this study, low-field NMR was used to measure the SFCC of two sandy samples with different particle sizes and three clayey samples with different dry densities. According to NMR results, the different freezing properties of adsorptive, capillary, and bulk water were investigated. In addition, a commonly used SFCC model was used to fit the measured data and the model performance was evaluated.

2 MATERIALS AND METHODS

This section introduces the principle of NMR tests in quantifying unfrozen water content and identifying different types of soil water. And then the sample preparation and test procedure are described in detail.

2.1 Theoretical background of NMR

A proton has a magnetic moment. Hence, a water molecule with two protons can be regarded as a magnet. If a soil sample with water is embedded in an external magnetic field, all water molecules tend to align in the direction of the magnetic field. Therefore, these water molecules form an initial magnetization. This phenomenon can be described by the following equation (Tian et al., 2017):

$$M_0 = CNB_0/T \qquad (1)$$

where B_0 is the external magnetic field, T is temperature, N is the number of water molecules, M_0 is the initial magnetization, and C is a constant parameter. Eq. (1) illustrates the amplitude of M_0 is proportional to the water mass and can be used to quantify soil water content. Ice can not be detected by NMR, hence the unfrozen water content w_u can be calculated by the following equation according to Eq. (1):

$$w_u = w_0(TM_0(T))/ (T_0M_0(T_0)) \qquad (2)$$

where w_0 is the initial water content at a referenced temperature T_0. Utilizing Eq. (2) the influences of temperature on magnetization also can be eliminated.

Under the static external magnetic field, if a magnetic pulse is exerted, the magnetization will orientate in a new direction. Then, once the magnetic pulse is removed, water molecules will return to the initial position, the process of which is called relaxation and can be described by

$$M(t) = M_0\exp(-t/T_2) \qquad (3)$$

where t is time, T_2 is the transverse relaxation time, and M is the magnetization that can be captured by the equipment. Protons in different environmental conditions have different T_2 values. For example, the T_2 of protons in ice is too short to be detected; the soil-water interactions are able to accelerate relaxation and result in a shorter T_2 value; and bulk water has a longer relaxation time than water affected by the environment. Therefore, the T_2 of soil water is a distribution curve due to the existence of several types of soil water. The NMR measurement can give the T_2 distribution curve by analyzing the NMR signal variation with an inversion algorithm.

2.2 Sample preparation

In order to analyze the connections between soil properties and SFCCs, a total of five different samples were prepared, which are summarized in Table 1. S1 and S2 are glass beads with different particle sizes representing different sandy soil. S3a, S3b, and S3c are high-purity kaolin (K299133, Shanghai Aladdin Biochemical Technology Co., Ltd) with different dry densities.

The sample powder was compacted into a Teflon mold after a drying process of eight hours at 105 °C. The mold is a cylinder with a height of 4 cm and a bottom diameter of 1.6 cm. The mold made by Teflon can avoid magnetic substances disturbing the NMR tests. Samples were saturated by the vacuum saturation method. Samples were placed in a closed container and a vacuum pump was operated for 2 hours. Then, deionized water was injected until the sample was submerged. Next, the vacuum was removed and the samples were saturated for one day.

The saturated samples were sealed with plastic film and then stored in a temperature controlled container. The measured temperature points include 25, 20, 15, 10, 5, 0, -1, -1.5, -2, -2.5, -3, -3.5, -4, -4.5, -5, -7,-10, and -20°C. The samples were stored in the container for at least 4 hours under a certain temperature point before the NMR test to achieve the temperature equilibrium. The NMR test procedure was completed in a few minutes to assure that the temperature equilibrium was held.

Table 1. *Basic properties of the samples in this work*

Sample ID	Material	Particle size distribution	Dry density (g/cm3)	Saturated water content (g/g)
S1	Glass bead	600 μm[a]	1.459	0.248
S2	Glass bead	178 μm[a]	1.478	0.256
S3a	Kaolin	8.2μm (d_{60}),4.5μm (d_{30}), 2.1μm (d_{10})	0.880	0.704
S3b			0.929	0.638
S3c			0.998	0.569

[a] Indicating all the particles can pass the sieve of this value.

2.3 NMR measurements

A 2MHz low-field NMR equipment was utilized in this study (0.3 ± 0.05 T, Suzhou Niumag Analytical Instrument Corporation, China). The NMR test used the CPMG pulse sequence (Carr & Purcell, 1954; Meiboom & Gill, 1958). CPMG consists of a series of magnetic pulses. The first pulse in the CPMG rotates the water molecules 90° from the initial B_0 direction. And then a series of equally spaced 180° pulses are exerted. In the CPMG test process, water molecules return a series of signals and the transverse relaxation time can be obtained from them. The echo spacing time was 0.1 ms. The number of echoes is 8000. After all the measurements, the measured data were analyzed to generate the T_2 distribution curves using the SIRT inversion procedure provided by Suzhou Niumag.

3 RESULTS AND DISCUSSION

NMR provided the SFCCs and T_2 distributions of different samples, laying the data foundation for furtherly analyzing the different roles of different types of soil water in the soil freezing process.

3.1 Variation of the unfrozen water content with temperature

The unfrozen water contents determined from the NMR test and Eq. (2) are illustrated in Figure 1. All SFCCs can be divided into three stages. In the first stage, the unfrozen water content almost no changes with temperature decreasing, which is known as the supercooling phenomenon. The supercooling phenomenon is common in nature. If a new phase is generated in an old phase, the new phase needs to grow from a small nucleus. The smaller the nucleus size, the higher the surface energy required to overcome. The probability of initial nucleus formation is very small due to the high surface energy. Therefore, the initial formation of ice in water is difficult even the temperature has reached the freezing point (Wang et al., 2021). Supercooling water is in an unstable state and will transform into ice under disturbances, which is hard to be predicted in practice. In the second stage, the unfrozen water content steeply decreases within the temperature range of narrower than 1 °C. A large part of unfrozen water changes into ice in this stage. Finally, in the third stage, the residual unfrozen water is gradually frozen.

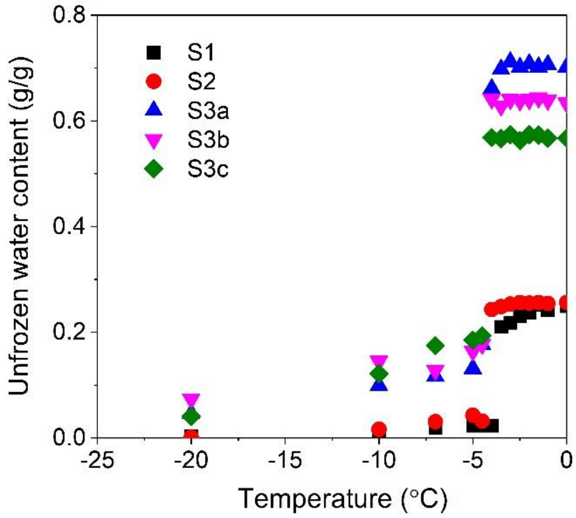

Figure 1. *Measured soil freezing characteristic curves for different samples.*

Although the three stages can be observed in all SFCCs, the SFCCs of different samples are significantly different. The unfrozen water content of S1 is the least in all temperature points, and the unfrozen water content of S2 is the second least. Clayey samples contain much more unfrozen water contents than sandy samples.

For the three clayey samples, the water content of S3a is the most in the first stage due to its high saturation water content. However, the unfrozen water content of S3a is the least in the three clayey samples in the third stage. This transition can be explained by the PSD. The materials of the three clayey samples are the same, meaning their SSAs are identical. Nonetheless, the dry densities of the three samples are different. The dry density of S3a is the smallest. Hence, the void ratio and average pore size of S3a are larger than these of S3b and S3c. Pore structures control the properties of capillary water. The water in the smaller pores is more difficult to freeze (Wang et al., 2022a), which causes the unique variation in the unfrozen water content of clayey samples.

Generally, SSA is proportional to the adsorptive water content (Tuller & Or, 2005), and the freezing point of adsorptive water is lower than that of capillary water and bulk water. In all tested samples, the SSA of S1 is the smallest, followed by S2. The clayey sample has a much higher SSA according to the particle size data. The unfrozen water content in the third stage shows good consistency with the SSA sequence, proving the adsorptive water content is the main component of the total unfrozen water content in the third stage. At the temperature of -20 °C, the capillary water has almost been frozen completely. The unfrozen water contents of the three clayey samples are close because only adsorptive water can exist at this temperature and their identical SSAs indicate that their adsorptive water contents are close.

3.2 Variation of the T_2 distribution with temperature

SFCCs only provide information on total unfrozen water content. The details of soil water components can be revealed by analyzing the T_2 distribution. Figure 2 demonstrates the T_2 distributions of different samples at four temperature points. The area under the T_2 curve is proportional to the water content. At the temperature of 0 °C, all soil water remains liquid, but their T_2 distributions are different. The average T_2 value of S1 is longer than that of S2, and both of them are longer than that of clayey samples. According to previous studies, the T_2 value of bulk water should be larger than 10 ms, capillary water should be in the range of 1 ~ 10 ms, and adsorptive water should be smaller than 1 ms (Chen et al., 2021). Therefore, the water in S1 and S2 should mainly be bulk water. The T_2 curves of S1 and S2 disappear suddenly, e.g., the T_2 curve of S2 barely changes from 0 °C to -4 °C and disappears completely at -4.5 °C. Once the bulk water reaches its supercooling limit, it freezes completely. Hence S1 and S2 almost have no NMR signals. For clayey samples, the T_2 variations with temperature are more complex. At 0 °C, the lower the dry density, the longer the T_2 value. Based on the results of S1 and S2, it can be concluded that the small average pore size can accelerate the transverse relaxation. With the temperature decreasing, the T_2 values become shorter, and the signal intensity decrease, indicating a large part of the water is frozen and the remained water mainly is adsorptive water.

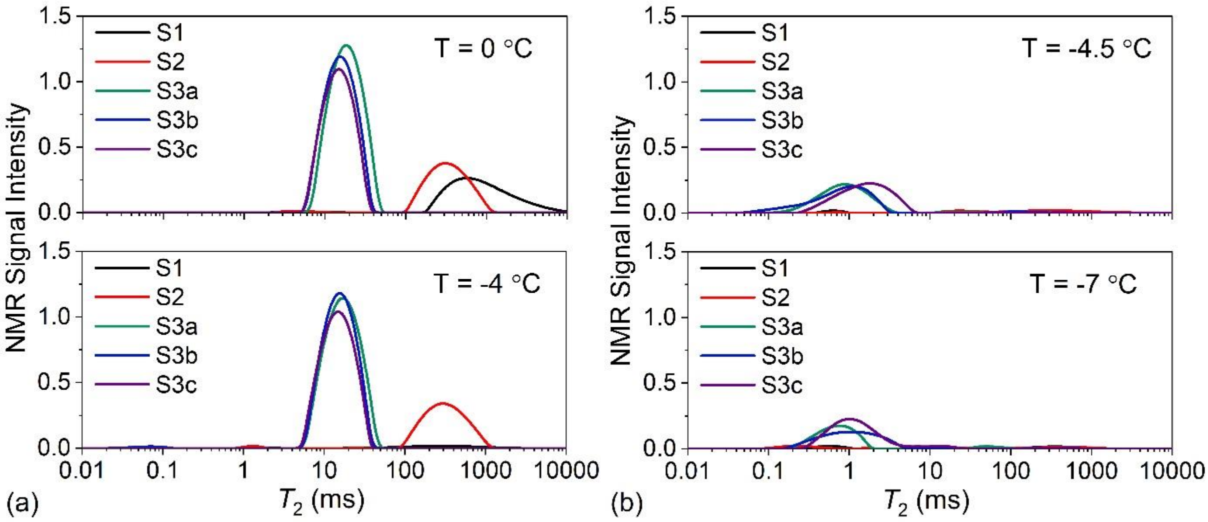

Figure 2. *The transverse relaxation time of different samples at the temperature of (a) 0 °C and -4°C; and (b) -4.5 °C and -7 °C.*

Figure 3 illustrates the detailed T_2 distribution variations with temperature for each sample. All curves have an obvious main peak, and this work regards the weak signal outside the main peak as the experimental noise and ignores them in the following analysis. The complete freezing process is divided into three stages in the last subsection. The first temperature point of the third stage represents that the bulk water has disappeared. Therefore, the T_2 distribution at this temperature point can be used to determine the shortest T_2 value of bulk water. The first temperature point of the third stage is -4 °C for S1 and -4.5 °C for other samples. And the maximum T_2 value in all these temperature points is 7 ms (S3a), indicating that the T_2 cutoff value between capillary water and bulk water must be higher than 7 ms. The three clayey samples S3a, S3b, and S3c are only different from PSD, indicating the amount and physical properties of their adsorptive water are very close. At the temperature of -20 °C, their total unfrozen water contents are nearly equal denoting the complete freeze of capillary water. Hence the T_2 cutoff value between adsorptive water and capillary water can be obtained from the T_2 distribution at -20 °C. At this temperature, the maximum T_2 values of S3a, S3b, and S3c are 1.3, 1.1, and 0.9 ms, respectively, indicating the T_2 cutoff value between adsorptive water and capillary water must be higher than 1.3 ms.

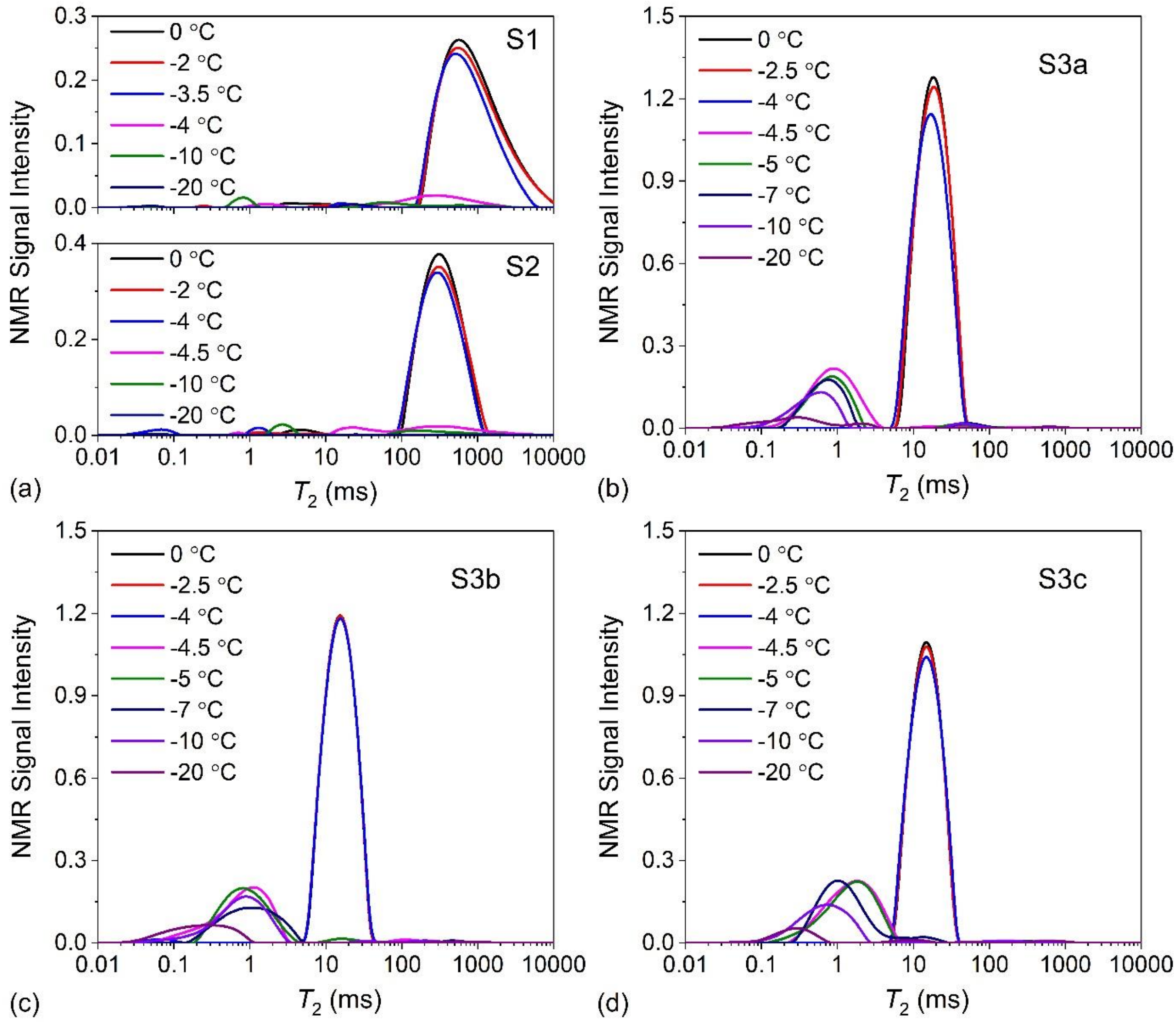

Figure 3. *The transverse relaxation time variations with the temperature: (a) S1 and S2; (b) S3a; (c) S3b; and (d) S3c.*

3.3 SFCC model fitting

SFCC models are commonly used in the numerical calculation of freezing soil problems, most of which ignore the difference between different types of soil water in the freezing process. This work fitted the experimental data with a simple power law SFCC model (Zhang et al., 2017) to evaluate the influence caused by the neglect of soil water components. This model can be formulated as follows,

$$w_u = w_0\left(1-\left((T_f-T)/(273.15+T_f)\right)^{\omega}\right) \quad T<T_f \qquad (4)$$
$$w_u = w_0 \quad T>=T_f$$

where w_0 is the initial water content, T_f is the initial freezing temperature of pore water (°C), and ω is a characteristic parameter of soil.

Table 2. *Fitted parameters for the SFCC model.*

Sample ID	w_0 (g/g)	T_f (°C)	ω
S1	0.208	-4.3	0.018
S2	0.253	-4.2	0.023
S3a	0.699	-4.4	0.035
S3b	0.638	-4.0	0.053
S3c	0.569	-4.2	0.063

All fitted parameters are summarized in Table 2, and the fitted SFCCs are visible in Figure 4. In general, the power law SFCC model can well describe the trend of unfrozen water content variation in the freezing process. However, the fitted curves are not very accurate due to the lack of soil water components division. For example, the low descent of the unfrozen water content in the temperature range of 0 °C to -4 °C of S1 can not be simulated; and the unfrozen water content variation in the third stage of S3c can not be fitted accurately. Therefore, it is necessary to consider the different roles of different types of soil water in the freezing process if the computational power is sufficient.

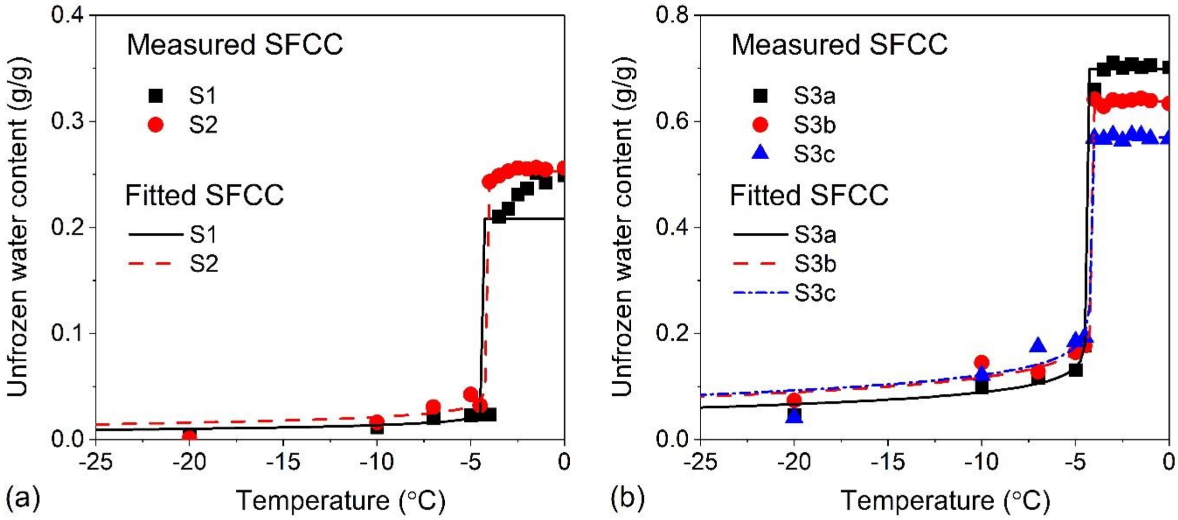

Figure 4. *Fitted and measured SFCC curves of (a) S1 and S2; and (b) S3a, S3b, and S3c.*

4 CONCLUSIONS

This study performed a series of NMR tests on different soil samples equilibrated at different subzero temperatures to measure the SFCCs and T_2 value distributions. According to the measurement results, the different roles of adsorptive, capillary, and bulk water during the freezing process were investigated, and the performance of a power function SFCC model was evaluated.

Some findings are summarized as follows: (1) Soil properties, i.e., SSA and PSD, dominate the variation of unfrozen water content in the freezing process by controlling the adsorptive water content, capillary water content, and bulk water content in the soil; (2) Bulk water freezes first, followed by capillary water, and adsorptive water during a cooling process; (3) The supercooling phenomenon controls the onset of the soil water freezing; (4) The T_2 cutoff value between capillary water and bulk water is longer than 7 ms, and the value between adsorptive water and capillary water is longer than 1.3 ms; (5) The roles of different types of soil water should be adequately considered to develop a more accurate SFCC model.

5 ACKNOWLEDGEMENTS

This research is supported by the National Natural Science Foundation of China (51979144) and the National Key Research and Development Program of China (2020YFC1806502).

REFERENCES

Carr, H. Y., & Purcell, E. M. (1954). Effects of Diffusion on Free Precession in Nuclear Magnetic Resonance Experiments. Physical Review, 94(3), 630-638.

Chen, Y., Zhou, Z., Wang, J., Zhao, Y., & Dou, Z. (2021). Quantification and division of unfrozen water content during the freezing process and the influence of soil properties by low-field nuclear magnetic resonance. Journal of Hydrology, 602, 126719.

Job, G., & Herrmann, F. (2006). Chemical potential—a quantity in search of recognition. European Journal of Physics, 27(2), 353-371.

Meiboom, S., & Gill, D. (1958). Modified Spin-Echo Method for Measuring Nuclear Relaxation Times. Review of Scientific Instruments, 29(8), 688-691.

Teng, J., Kou, J., Yan, X., Zhang, S., & Sheng, D. (2020). Parameterization of soil freezing characteristic curve for unsaturated soils. Cold Regions Science and Technology, 170, 102928.

Tian, H., Wei, C., Lai, Y., & Chen, P. (2017). Quantification of Water Content during Freeze–Thaw Cycles: A Nuclear Magnetic Resonance Based Method. Vadose Zone Journal, 17(1), 1-12.

Tuller, M., & Or, D. (2005). Water films and scaling of soil characteristic curves at low water contents. Water Resources Research, 41(9).

Wang, C., Li, S., Lai, Y., Chen, Q., He, X., Zhang, H., & Liu, X. (2022a). Predicting the Soil Freezing Characteristic From the Particle Size Distribution Based on Micro-Pore Space Geometry. Water Resources Research, 58(1).

Wang, C., Wu, J., Wang, H., & Zhang, Z. (2021). Classical nucleation theory of ice nucleation: Second-order corrections to thermodynamic parameters. J Chem Phys, 154(23), 234503.

Wang, Y., Hu, L., Luo, S., & Lu, N. (2022b). Soil water isotherm model for particle surface sorption and interlamellar sorption. Vadose Zone Journal, e20221.

Zhang, C., & Lu, N. (2021). Soil Sorptive Potential–Based Paradigm for Soil Freezing Curves. Journal of Geotechnical and Geoenvironmental Engineering, 147(9), 04021086.

Zhang, M., Pei, W., Li, S., Lu, J., & Jin, L. (2017). Experimental and numerical analyses of the thermo-mechanical stability of an embankment with shady and sunny slopes in a permafrost region. Applied Thermal Engineering, 127, 1478-1487.

The paper was published in the proceedings of the 9th International Congress on Environmental Geotechnics (9ICEG), Volume 3, and was edited by Tugce Baser, Arvin Farid, Xunchang Fei and Dimitrios Zekkos. The conference was held from June 25th to June 28th 2023 in Chania, Crete, Greece.